Outer Membrane Vesicles from bacteria expressing the HlyF/CprA family of enzymes are more efficient at delivering their cargo into host cells.

Frédéric Taieb[a#*], Laure David[a#], Camille Pin[a], Audrey Goman[a], Asja Garling[a], Marine Colson[a], Marie Pénary[a], and Eric Oswald[a,b*]

[a]Institut de Recherche en Santé Digestive (IRSD), Université de Toulouse, INSERM, INRAE, ENVT, UPS, Toulouse, France; [b]Service de Bactériologie-Hygiène, Centre Hospitalier Universitaire de Toulouse, Hôpital Purpan, France

# These authors contributed equally

*Address correspondence to: eric.oswald@inserm.fr; frederic.taieb@inrae.fr

Keywords: Outer Membrane Vesicle, HlyF, CprA, *Escherichia coli, Pseudomonas aeruginosa*

Abbreviations:

AUC: area under the curve

CtxB: cholera toxin B

E. coli: *Escherichia coli*

EHEC: enterohemorrhagic *E. coli*

ETEC: enterotoxigenic *E. coli*

FRET: fluorescence resonance energy transfer

HBSS: Hanks' balanced salt solution

HlyF: hemolysin F

LPS: lipopolysaccharide

mut: mutated

M/PAMPs: microbial/pathogen-associated molecular patterns

NMEC: neonatal meningitis associated *E. coli*

OMPs: outer membrane proteins

OMVs: outer membrane vesicles

P. aeruginosa: *Pseudomonas aeruginosa*

SDR: short chain dehydrogenase/reductase

TEM: transmission electron microscopy

UPEC: uropathogenic *E. coli*

wt: wild-type

Abstract

HlyF, a cytoplasmic short-chain dehydrogenase/reductase (SDR) enzyme encoded by a virulence plasmid in *Escherichia coli*, and its ortholog CprA, encoded by the chromosome of *Pseudomonas aeruginosa*, drive the production of specific outer membrane vesicles (OMVs). These OMVs have been shown to have the unique abilities to disrupt autophagic flux and exacerbate inflammatory response in host cells. In this study, we demonstrate that these OMVs have improved cargo delivery efficiency through a clathrin-independent pathway by direct fusion of the vesicle with the plasma membrane of the host cell. These results reveal an uncovered role of the HlyF/CprA enzyme family in enhancing OMV function through a unique internalization pathway and unveil a novel mechanism driving OMV-mediated virulence.

Introduction

Gram-negative bacteria, as all cells, release extracellular vesicles (EVs). Among various subtypes, EVs that bud from their outer membrane are called outer membrane vesicles (OMVs). These nanoparticles convey a variety of molecular components originating from both the outer membrane and the periplasm of the parent bacteria. These molecules include lipids, lipopolysaccharides (LPS), outer membrane proteins (OMPs) and periplasmic compounds including toxins [1-3]. By exposing surface pro-inflammatory antigens and microbial/pathogen-associated molecular patterns (M/PAMPs), OMVs modulate both innate and acquired immune responses, potentially triggering lethal sepsis in animal models [4, 5]. Many studies have demonstrated that eukaryotic cells can internalize bacterial vesicles by endocytosis, meaning that OMVs deliver into host cells, not only membrane components including lipids, OMPs, PAMPs, and LPS but also toxins and various periplasmic molecules, thus participating in the host-pathogen interaction [6, 7]. Therefore, OMVs are now recognized to play pivotal roles in various biological processes, particularly in the context of virulence. We have previously identified in pathogenic *Escherichia coli* strains a gene called *hlyF*, located on

a virulence plasmid, that encodes for an enzyme belonging to the short chain dehydrogenase/reductase (SDR) family [8-10]. Similarly, we identified *cprA* as a functional ortholog of *hlyF* located on the chromosome of *Pseudomonas aeruginosa* [10]. HlyF and CprA are cytoplasmic enzymes that induce the production of OMVs able to block the autophagic flux of intoxicated eukaryotic cells [10, 11]. As this flux contributes to the negative feedback loop of inflammasome activation, this OMV-dependent inhibition of autophagy results in the exacerbation of the non-canonical inflammatory response triggered by OMV-mediated PAMPs delivery, eventually leading to cell death [10-12]. The expression of HlyF and CprA has been further linked to pathogenicity of *E. coli* and *P. aeruginosa* in avian colibacillosis [8] and murine models of sepsis [10] or urinary tract infection, promoting pyelonephritis accompanied by bloodstream infection [9]. To explore how OMVs produced by HlyF/CprA SDR contribute to bacterial virulence, we investigated their mode of entry within eukaryotic cells. In this study, we demonstrate that these OMVs have improved cargo delivery efficiency into host cells. Our results revealed that HlyF/CprA induces enhanced entry of OMVs into the host cell via a clathrin-independent pathway by promoting their direct fusion with the host plasma membrane. This atypical and HlyF/CprA-dependent mode of internalization of OMV stimulates the delivery of their virulence factors into host cells, promoting bacterial pathogenicity.

Results

Production and characterization of OMVs produced by BL21(DE3) *E. coli* strains expressing functional or inactive HlyF together with TEM-1 ß-lactamase as cargo.

We have previously shown that cloning of genes encoding HlyF in BL21(DE3) strain enables the production of OMVs blocking the autophagic flux [11]. Therefore, BL21(DE3) *E. coli* strains were transformed with plasmids expressing either the wild-type HlyF ($HlyF^{wt}$) or an inactive form of HlyF mutated in the catalytic site ($HlyF^{mut}$) together with the high copy number pUC19 plasmid producing the ß-lactamase TEM-1, for further use as a reference cargo and to assess the efficiency of its internalization into host cells. This enzyme is translocated into the periplasmic space by the sec-system pathway where it acquires its native active form following the cleavage of the N-terminal signal peptide and oxidative folding [13]. Thus, OMVs, that embark periplasmic molecules, contain the enzyme TEM-1 as cargo (figure 1A, B). Microscopic observation of $HlyF^{wt}$ and $HlyF^{mut}$ OMVs revealed a consistent similar vesicle structure, as expected for OMV formation, along with similar apparent diameter sizes for both types of

OMVs (supplementary figure 1A). Subsequent assessment of OMV size distribution via dynamic light scattering (DLS) yielded comparable results for both HlyF^{wt} and HlyF^{mut} OMVs, with a mean diameter falling within the range of 21-24 nm (supplementary figure 1B). It is important to point out that the DLS technique allows accurate assessment of vesicle size which is below the detection limit of 50 nm for the nanoparticle tracking analysis (NTA) technology owing to the low refractive index of extracellular vesicle [14, 15]. Both types of OMVs exhibited a similar protein profile (supplementary figure 1C) and the same amount of TEM-1 ß-lactamase as quantified by western blot with the transmembrane protein OmpA used as a loading control (figure 1B). Together, these analyses showed that OMVs produced by HlyF-expressing and non-HlyF-expressing bacteria exhibit similar protein composition and structural and physical features.

<u>HlyF expression in BL21(DE3) *E. coli* strains enhances OMV's cargo accumulation into host cells</u>

To investigate the rate of cargo delivery in eukaryotic cells, we employed a reporter system based on β-lactamase activity, measured using the fluorescence resonance energy transfer (FRET) substrate CCF4-AM. This substrate consists of a cephalosporin core linking 7-hydroxycoumarin to fluorescein. Purified OMVs containing a normalized quantity of β-lactamase (validated by western blot, figure 1B) were added to HeLa cells preloaded with CCF4-AM. Cleavage of cephalosporin by β-lactamase TEM-1 disrupts CCF4-AM FRET, shifting fluorescence from green to blue (Figure 1C). Monitoring the blue/green fluorescence kinetics enables precise quantification of OMV cargo delivery over time (Figure 1D). The total β-lactamase TEM-1 level in host cells was quantified by calculating the area under the curve (AUC). AUC analysis revealed that addition of HlyF^{wt} OMVs resulted in a greater accumulation of ß-lactamase into HeLa cells compared to HlyF^{mut} OMVs (figure 1E). As shown in Figure 1F, the steeper slope of the green/blue fluorescence curve for HlyF^{wt} OMVs suggests that an accelerated rate of accumulation of the enzyme accounts for their greater overall delivery compared to HlyF^{mut} OMVs.

<u>OMVs from clinical isolates of pathogenic *E. coli* and *P. aeruginosa* strains expressing HlyF and CprA respectively, show enhanced cargo accumulation into host cells</u>

Our experiment showing that HlyF stimulated the accumulation of TEM-1 β-lactamase OMV cargo was first performed with OMVs from the laboratory strain BL21 (Fig. 1D, 1E, 1F). We next

confirmed these results using naturally *hlyF*-expressing *E. coli*. OMVs were purified from the SP15 strain, a neonatal bacterial meningitis-causing *E. coli* (NMEC) [16], expressing either wild-type $HlyF^{wt}$ or an inactive form of $HlyF^{mut}$ mutated in the SDR catalytic site [11] and from a clinical uropathogenic *E. coli* (UPEC) strain, ECC166 wild-type and its isogenic hlyF-deleted strains [9]. We extended our investigation using OMVs from *P. aeruginosa* PAK strain, a different bacterial specie expressing HlyF ortholog, CprA and the isogenic deleted strains [10]. All strains were transformed with TEM-1 ß-lactamase expressing plasmids (see material & method) and OMV concentration were normalized for equivalent enzyme load before addition on HeLa cells loaded with CCF4-AM. As observed with OMVs from BL21(DE3), AUC levels for OMVs produced by strains expressing active HlyF/CprA were higher compared to the corresponding *hlyF/cprA*-mutant strains suggesting that $HlyF^{wt}$/CprA OMVs resulted in a more massive accumulation of ß-lactamase TEM-1 into host cells than with $HlyF^{mut}$ OMVs or OMVs produced in absence of HlyF/CprA (figure 2A, B and C). Since all experiments were performed with pairs of OMVs containing identical quantities of ß-lactamase, these results demonstrate that OMVs derived from pathogenic HlyF/CprA-expressing bacteria (NMEC, UPEC and *P. aeruginosa*) as from BL21(DE3) promote faster and higher accumulation of their cargo into host cells.

<u>HlyF promotes enhanced delivery of OMV cargo into host cells.</u>

The increased AUC, which is dependent on ß-lactamase activity, observed with OMVs from hlyF/cprA-positive bacteria, suggested an improved vesicle internalization in host cells. Alternatively, given that $HlyF^{wt}$ OMVs have been shown to block host cell autophagy [11, 12], it can be hypothesized that an autophagic-dependent degradation of OMVs internalized into endosome (following endocytosis) [3, 17, 18] is also disrupted. This inhibition could lead to the stabilization of OMV's cargo, including TEM-1 β-lactamase, increasing CCF4-AM cleavage and thus increasing the associated AUC. To investigate this hypothesis, we used inhibitors of the autophagic flux, chloroquine and bafilomycin [19]. If the increased AUC were due to TEM stabilization induced by $HlyF^{wt}$ OMVs as a result of autophagic blockage [11], then, autophagic inhibitors would be expected to boost AUC in $HlyF^{mut}$ OMV-treated cells to the same level as that observed with $HlyF^{wt}$ OMVs. As shown in figure 3A and 3B, the addition of these pharmacological inhibitors did not lead to an increase in AUC, suggesting that the rise in ß-

lactamase activity is unrelated to autophagic dysfunction and instead results from enhanced OMV entry improving delivery of TEM-1 β-lactamase.

OMVs from bacteria producing HlyF^{wt} enter cell by a clathrin-independent pathway

To understand what are the enhanced delivery properties conferred by HlyF on OMVs, we focused on HlyF^{wt} and HlyF^{mut} OMVs produced by *E. coli* BL21(DE3) strain devoid of virulence gene. *E. coli*-derived OMVs have been reported to be internalized through both clathrin- and caveolin-dependent endocytosis [3, 17, 20-24]. The formation of both caveolin and clathrin vesicles requires the concerted intervention of several proteins allowing the deformation of plasma membrane to form an internal sack that will eventually be pinched off from the membrane by the polymerization of the GTPase enzyme dynamin, to be released into the cytoplasm as an early endosome [25, 26]. To further understand the HlyF-dependent mode of entry of OMVs, we used Dynasore, a dynamin GTPase inhibitor that blocks both clathrin and caveolin-dependent endocytosis pathways [27-29]. Cells loaded with CCF4 were treated or not with Dynasore and HlyF^{wt} or HlyF^{mut} OMVs with the same quantity of TEM-1 cargo. As previously reported for OMVs produced by bacteria that do not express *hlyF* [3, 17, 20-23], Dynasore blocked the entry of OMVs from *E. coli* expressing the inactive form of HlyF. Interestingly, despite a diminution of AUC compared to the condition without Dynasore, a significant fraction of HlyF^{wt} OMVs entry was still maintained in inhibitor-treated cells (figure 3C). It can be inferred that the partial ß-lactamase activity observed with HlyF^{wt} OMVs in the presence of Dynasore might be attributed to its higher activity without inhibitor. To rule out the possibility that the observed result was solely due to the increased ß-lactamase entry associated with HlyF^{wt} OMVs, we used 2.5 times less HlyF^{wt} OMVs to achieve an equivalent AUC in control cells (i.e. without inhibitor) for both types of OMVs. Once again, addition of Dynasore effectively blocked the entry of HlyF^{mut} OMVs by almost 80%. In contrast, this inhibition was almost abolished for HlyF^{wt} OMVs intoxicated cells as only 10% of the ß-lactamase activity was hindered in the presence of Dynasore (figure 3D). These results demonstrated that HlyF provides to OMV the ability to enter host cells independently of previously documented clathrin/dynamin endocytosis pathways. The observation that a higher dose of HlyF^{wt} OMVs resulted in a greater inhibition of internalization by Dynasore (50% in figure 3C) compared to a lower dose (10% in figure 3D) suggests that, at elevated vesicle

concentrations, the uptake of HlyF^{wt} OMVs partially relies on dynamin-dependent endocytosis once the dynamin-independent pathway reaches saturation.

HlyF promotes OMV internalization by direct fusion to host cell plasma membrane

We then analyzed the mode of internalization of HlyF^{wt} OMVs into eukaryotic cells. As lipid rafts microdomains of the plasma membrane were described to be required for *P. aeruginosa* OMVs fusion [30], we used cholera toxin B subunit labeled with FITC (CtxB-FITC), a documented lipid raft marker [31]. In the non-treated condition and in the condition treated by HlyF^{mut} OMVs, CtxB-FITC fluorescence was detected and clustered, as denoted by CtxB-FITC green patches. In contrast, clusters of CtxB-FITC in the cells treated with HlyF^{wt} OMVs were fewer in number and more diffusely distributed throughout the cell (figure 4). This result showed that HlyF^{wt} OMVs disrupted the clustering of CtxB-FITC associated lipid rafts. As separation of CtxB-FITC foci has been shown to be caused by lipid membrane dynamics [31], this observation suggests that membranes from HlyF^{wt} OMVs directly fuse with the host cell membrane, causing the destabilization of plasma membrane lipids and the dispersion of CtxB-FITC clusters.

Discussion

Here, we demonstrated that the cytosolic SDR enzymes HlyF/CprA promote the biosynthesis of bacterial vesicles that deliver their content more massively and rapidly in host cells compared to classical OMVs from *hlyF*-negative strain. To understand the difference of kinetic entry of OMVs, we further take advantage of our reporter system with CCF4-AM loading kit. In contrast to non-HlyF OMVs that entered cells via previously described clathrin dynamin-dependent pathway, we showed that CprA/HlyF^{wt} OMVs are internalized in host cells in presence of the dynamin pharmacological inhibitor Dynasore demonstrating that a clathrin/caveolin-independent process is being implemented to promote a highly efficient OMV entry. This internalization route contrasts with previous findings since it has been described that OMVs from *E. coli* strains enter host cells in a clathrin-caveolin endocytic pathway [1, 3, 7, 17, 18, 20-24, 32, 33]. To our knowledge, a dynamin-independent internalization pathway has never been described for *E. coli*'s OMVs uptake. Interestingly and consistent with our results, another study showed that OMVs from *P. aeruginosa* harboring

cprA, the *hlyF* functional ortholog, are internalized via a dynamin independent process and implicating the fusion of OMV with the host cell's membrane [30]. Our microscopic observation of the interaction between HlyF^{wt} OMVs and host plasma membrane using Ctx-B also suggested a similar mechanism of entry for *E. coli* OMVs. Therefore, in addition to their capacity to block autophagic pathway and exacerbate inflammation [10, 11], these pathogenic vesicles reveal a new competence to enhance the delivery of their cargo into host cells.

We have recently shown that HlyF/CprA are SDR enzymes able to modify lipids present in the OMVs membrane, conferring them pathogenic properties [10]. These SDR-modified lipids could also explain their increased ability to fuse with cell membranes.

Additionally, we demonstrated that clinical pathogenic *E. coli* strains like NMEC (SP15) and UPEC (ECC166), as well as the opportunistic *P. aeruginosa* strain expressing HlyF/CprA, produce OMVs with similarly enhanced delivery capacity. The virulence plasmid coding for HlyF is also found in the enterohemorrhagic *E. coli* (EHEC) strain of serotype O80:H2, the actual second leading cause of pediatric hemolytic and uremic syndrome (HUS) in France [34, 35] and in the NMEC strain IHE3034 that also expresses the genotoxin cytolethal distending toxin (CDT) [8]. The fact that toxins such as the Shiga toxin Stx or CDT are present into OMV exhibiting increased delivery capacity could contribute to bacterial virulence. This HlyF/CprA-dependent increase of OMV cargo delivery could also be aggravated by the fact that LPS, PAMPs or toxins delivered by OMV could be stabilized since the autophagy-dependent degradation pathway is impaired as HlyF^{wt} OMVs or CprA OMVs are known to inhibit lysosome-autophagosome fusion [11, 12]. Additionally, fusion of OMV with the plasma membrane implies free release of their cargo in the host cytoplasm, potentially facilitating direct interaction of bacterial effector with eukaryotic cellular targets. These deleterious effects could worsen the clinical outcome of infection with *hlyF*/*cprA* positive bacteria as demonstrated in various experimental models of infection [8-10]. In addition to *cprA*, present in the core genome of *P. aeruginosa*, functional orthologs of *hlyF* were also found in other pathogens such as *Yersinia pestis* and *Ralstonia solanacearum* [10]. The wide distribution of this SDR gene among Gram-negative bacteria, which lead to the production of OMVs with new ability to enter host cells, might reveal an underestimated, as yet little-studied virulence weapon to hijack host signaling pathways for pathogen benefit.

Among all EVs in living organism, OMVs are unique due to the diderm organization of Gram-negative bacteria and their cargo, which originates specifically from the periplasm. These

vesicles have to be differentiated from outer-inner membrane vesicle (O-IMV) or membrane vesicle resulting from bacterial lysis (explosive membrane vesicle) that are different not only at the organization and structural level but also due to the origin and composition of their content. Among the diversity of EVs, we focused on OMVs, which are vesicles naturally secreted in the absence of bacterial stress or danger signals. However, their production and toxicity could be enhanced by HlyF/CprA probably via their SDR-dependent lipid modifications which promote an alternative pathway for OMV entry into host cells. Although often overlooked, these vesicles contribute to bacterial virulence including sepsis [8-10] and possibly to significant long-term and chronic pathogenic effects.

The elucidation of the OMV entry pathways highlights, beyond the presence or level of expression of particular virulence factors, the importance of the mode of uptake and trafficking of OMV into the host cell, to directly cause cellular injuries and ultimately contribute to bacterial virulence. Understanding the diversity of OMV and their interactions with host cells is critical to adapt and develop strategy to prevent OMV-dependent intoxination (even after potential eradication of the pathogen) and to, eventually, design avenue to fight bacterial pathogenesis.

Materials and methods

Bacterial strains and growth conditions

SP15 is an ExPEC strain isolated from a neonatal meningitis case [16]. SP15, SP15*Δhlyf* HlyF^{wt} and SP15*Δhly*F HlyF^{mut} were previously described in [8]. BL21(DE3) expressing wild-type and mutated HlyF were obtained following transformation with respectively, plasmids pAGO-15 and pAGO-16 previously described in [10]. BL21(DE3) strains were further transformed with pUC19 plasmid (Addgene). ECC166 is an uropathogenic *E. coli* strain (UPEC) isolated from woman with pyelonephritis. ECC166 and ECC166 Δ*hlyF* strains described in [9] were further transformed with pUC19 plasmid. *P. aeruginosa* PAK *ΔcprA* and PAK *ΔcprA* complemented with CprA strains were previously described in [10]. PAK strains were further transformed with pJN-TEM plasmid in which the tem-1 gene from pUC19 was inserted into the EcoRI-XbaI sites of pJN105 plasmid (Addgene) under the control of AraBAD promoter. For OMV production, bacteria were grown at 37°C under vigorous shaking (240rpm) for 8hr in M63 medium supplemented with casamino-acid and appropriate antibiotic and inoculated with 1/100 of

overnight culture. For PAK strains, 1% rhamnose and 1% arabinose were added after 3hr of culture for CprA and TEM-1 induction respectively.

Purification of bacterial OMVs

After 8hr of culture the bacterial suspension was centrifuged at 6500g for 10min at 4°C. The supernatant was filtered (pore size 0.45 µm; Merck-Millipore) to obtain bacterial-free supernatant. The filtered supernatant was ultrafiltered and concentrated using tangential concentrator and PES membrane cassette (pore size 100kDa; Sartorius) and then ultracentrifuged at 150,000g for 2hr at 4°C. After removing the supernatant, pelleted OMV were resuspended in sterile PBS with Ca^{2+} and Mg^{2+} and stored at 4°C. To visualize the concentration of OMVs and the purity of the preparation, negative staining transmission electron microscopy (TEM) was performed according to standard procedures. The concentration of OMVs in the suspension correlates with protein concentration evaluated by BCA protein assay (Bio-Rad, RC DCTM Protein Assay kit II). OMV diameter was calculated by dynamic light scattering using Zetasizer Nano instrument (Malvern).

Eukaryotic cell culture

HeLa cells (ATCC, HeLa CCL2) were cultured in DMEM with Glutamax (Life Technology) supplemented with 10% fetal bovine serum (FBS) and non-essentials amino-acids (Life Technology). One day before the experiment, HeLa cells were seeded in 96-wells plate at a density of 10^4 cells per well in 100µL of DMEM supplemented with 10% FBS. Bone marrow-derived macrophages (BMDM) were prepared from fresh bone marrow isolated from C57BL/6 mice. Bone marrow cells were allowed to differentiate in macrophages by incubation for 7 days in DMEM supplemented with 10% FBS, 25ng/ml CSF1/M-CSF (Immunotools), 10mM HEPES, pH 7.2 and nonessential amino acids (Life Technology). One day before treatment, BMDM were seeded into 96-well plates at a density of 2.5×10^5 cells per well in 100µL of DMEM supplemented with 10% FBS.

CCF4-AM assays

Twenty µL of 6X loading solution with CCF4-AM (LiveBLAzer FRET-B/G loading kit; Life technologies) supplemented with 2.5mM of probenicid were added to 100µL of cell culture in p96-well plate seeded at day-1 and further incubated at room temperature for 2hr. Cells were rinsed 3X with 100µl of HBSS and incubated with indicated concentration of OMVs in OptiMEM medium with probenicid. When indicated, Dynasore (80µM), chloroquine (100µM) or bafilomycin (100nM) were added together with OMVs. Background control wells without

CCF4, with and without inhibitors were performed. Each condition was done in triplicate. Plate reading was performed with Tecan Infinite 200 Pro (Tecan) at 37°C, every 15 minutes during 8hrs with excitation set at 410nm and detection of emission at 450nm (blue fluorescence) and 520nm (green fluorescence). CCF4-AM cleavage was calculated by the ratio of the net blue fluorescence (- background) divided by the net green fluorescence.

Immunoblotting

Detection of OmpA and ß-lactamase were performed with 2 µg of purified OMVs preparation per lane, separated by SDS-PAGE (Invitrogen) and transferred to PVDF membranes (Invitrogen). The membranes were blocked in 5% non-fat dry milk in TBS 0.1% Tween® 20 and probed with rabbit anti *E. coli* OmpA antibody (Antibody Research Corporation) and mouse anti-beta lactamase antibody [8A5.A10] (Abcam). After incubation with goat anti-rabbit and goat anti-mouse HRP-conjugated secondary antibodies (Bethyl Laboratories), proteins were visualized using chemiluminescent peroxidase substrate detection reagents (Sigma), and acquired by the ChemiDoc XRS+ System (Bio-Rad). Protein quantification was performed by densitometric analyses of immunoblots using the ImageJ software.

Fluorescence microscopy

HeLa cells were seeded at a density of 5×10^5 cells per well in 1mL of DMEM supplemented with 10% FBS into 12 wells plates with slides in the bottom of the wells the day before the experiment. The day of the experiment, cells were treated with 10µg/mL of OMV for 1,5 hours. CtxB-FITC (Sigma, C1655) was added directly in the medium of cell culture at a final concentration of 1µg/mL at the same time as OMV. At the end of the experiment the cells were fixed with 4% PFA for 12 minutes at RT. After being washed 3 times with PBS the slides were mounted with Fluoroshield (sigma F6182). Images were acquired using a Zeiss LSM 710 confocal microscope. Images were subsequently processed using the ImageJ software package.

Statistical analyses

Statistical analyses were performed on at least three independent experiments with the unpaired t-test using the Prism software package (GraphPad Software). Differences were considered significant for the following P-values: *P<0.05; **P<0.01; ***P<0.001; ****P<0.0001.

Figure legends:

Figure 1: HlyF stimulates TEM-1 ß-lactamase accumulation into eukaryotic cells. A: Schematic representation of production of OMV containing TEM-1 ß-lactamase: BL21 bacteria transformed with plasmid encoding TEM ß-lactamase and plasmid expressing either HlyF wild-type (wt) or HlyF mutated (mut), produce OMV containing ß-lactamase and OmpA (grey barrel). B: Western blot detection of OmpA and TEM-1 ß-lactamase from 0.5µg of purified OMV from BL21 strains expressing mut or wt HlyF. C: Principle of detection of OMV-mediated delivery of ß-lactamase into host cells: intact CCF4 probe emits green fluorescence and following its cleavage by ß-lactamase delivered by internalized OMV, CCF4 emits blue fluorescence due to loss of FRET. D: Time course experiment showing blue/green fluorescence ratio in HeLa cells treated with indicated concentration of OMV (representative of triplicate experiment and errors bars represent standard error of the mean). E: Quantification of TEM-1 ß-lactamase in host cells was evaluated by area under the curve (AUC calculated from D graph) of 4 independent experiments with 10µg/mL of indicated OMV (errors bars represent standard error of the mean; ANOVA test with Bonferroni correction: * $p<0.05$, ** $p<0.01$, *** $p<0.001$). F: The slope was determined by simple linear regression of blue/green fluorescence curves from D graph.

Figure 2: OMVs from clinical pathogenic strains expressing HlyF/CprA promote cargo accumulation into host cells. Area under the curve (AUC) representing total delivery of OMV-associated TEM-1 ß-lactamase were calculated from time course experiment as shown in figure 1D with A: 10µg/mL of OMV from SP15Δ*hlyF* bacteria expressing either mutated (mut) or wild-type (wt) HlyF; B: 10 and 20µg/mL of OMV from ECC166 *ΔhlyF* (black bar) or wt (white bar) strains; C: 10, 20 and 30µg/mL of OMV from PAK *ΔcprA* (black bar), PAK *ΔcprA* complemented with *cprA* (white bar). Errors bars represent standard error of the mean.

Figure 3: Evaluation of entry of OMV produced by BL21(DE3) expressing wild-type or inactive HlyF in presence of pharmacological inhibitors. AUC were determined for cells treated with 10µg/mL of $HlyF^{mut}$ OMV or $HlyF^{wt}$ OMV from BL21(DE3) in presence of DMSO (white bar) and pharmacological inhibitors (grey bar) A: chloroquine (+CQ); B: bafilomycin (+Baf); C: Dynasore (+Dyn); D: AUC were evaluated from 3 independent experiments with $HlyF^{wt}$ OMV (2µg/mL)

or $HlyF^{mut}$ OMV (5µg/mL BL21 (DE3) in presence (Dyn) or absence (DMSO) of dynasore. AUC were expressed as percentage of condition $HlyF^{wt}$ OMV + DMSO. Errors bars represent standard error of the mean; ANOVA test with Bonferroni correction: ns: non significative; ****: $p<0.01$; ****: $p<0.001$

Figure 4: OMV HlyF wt are internalized by direct fusion to host cell plasma membrane. Images of confocal microscopy of cholera toxin B subunit labeled with fluorescein isothiocyanate (CtxB-FITC)(green) and of nuclei (DAPI) in HeLa cells treated 1h30 with 5 µg/mL of BL21(DE3) $HlyF^{wt}$ OMV or $HlyF^{mut}$ OMV. Scale bar: 10µm. Images representative of 5 independent experiments.

Supplementary figure 1: Characterization of OMV produced by BL21(DE3) expressing wild-type or mutated HlyF. A: Negative staining transmission electronic microscopy of purified $HlyF^{mut}$ and $HlyF^{wt}$ OMVs (scale bar: 100nm); B: Measurement of OMV diameter by dynamic light scattering; C: silver (left) and coomassie blue (right) staining of $HlyF^{mut}$ and $HlyF^{wt}$ OMV proteins runed on SDS-PAGE

References:

1. Schwechheimer C, Kuehn MJ. Outer-membrane vesicles from Gram-negative bacteria: biogenesis and functions. Nature reviews Microbiology. 2015;13(10):605-19. doi: 10.1038/nrmicro3525. PubMed PMID: 26373371.
2. Juodeikis R, Carding SR. Outer Membrane Vesicles: Biogenesis, Functions, and Issues. Microbiol Mol Biol Rev. 2022;86(4):e0003222. Epub 20220926. doi: 10.1128/mmbr.00032-22. PubMed PMID: 36154136; PubMed Central PMCID: PMCPMC9881588.
3. Bielaszewska M, Ruter C, Bauwens A, Greune L, Jarosch KA, Steil D, et al. Host cell interactions of outer membrane vesicle-associated virulence factors of enterohemorrhagic Escherichia coli O157: Intracellular delivery, trafficking and mechanisms of cell injury. PLoS Pathog. 2017;13(2):e1006159. doi: 10.1371/journal.ppat.1006159. PubMed PMID: 28158302; PubMed Central PMCID: PMC5310930.
4. Eren E, Planes R, Bagayoko S, Bordignon PJ, Chaoui K, Hessel A, et al. Irgm2 and Gate-16 cooperatively dampen Gram-negative bacteria-induced caspase-11 response. EMBO Rep. 2020;21(11):e50829. Epub 20201030. doi: 10.15252/embr.202050829. PubMed PMID: 33124769; PubMed Central PMCID: PMCPMC7645206.
5. Park KS, Choi KH, Kim YS, Hong BS, Kim OY, Kim JH, et al. Outer membrane vesicles derived from Escherichia coli induce systemic inflammatory response syndrome. PloS one. 2010;5(6):e11334. doi: 10.1371/journal.pone.0011334. PubMed PMID: 20596524; PubMed Central PMCID: PMC2893157.
6. Pathirana RD, Kaparakis-Liaskos M. Bacterial membrane vesicles: Biogenesis, immune regulation and pathogenesis. Cellular microbiology. 2016. doi: 10.1111/cmi.12658. PubMed PMID: 27564529.
7. Sabatke B, Rossi IV, Sana A, Bonato LB, Ramirez MI. Extracellular vesicles biogenesis and uptake concepts: A comprehensive guide to studying host-pathogen communication. Molecular microbiology. 2024;122(5):613-29. Epub 20230927. doi: 10.1111/mmi.15168. PubMed PMID: 37758682.
8. Murase K, Martin P, Porcheron G, Houle S, Helloin E, Penary M, et al. HlyF Produced by Extraintestinal Pathogenic Escherichia coli Is a Virulence Factor That Regulates Outer Membrane Vesicle Biogenesis. The Journal of infectious diseases. 2016;213(5):856-65. doi: 10.1093/infdis/jiv506. PubMed PMID: 26494774.
9. Chagneau CV, Payros D, Goman A, Goursat C, David L, Okuno M, et al. HlyF, an underestimated virulence factor of uropathogenic Escherichia coli. Clin Microbiol Infect. 2023;29(11):1449 e1- e9. Epub 20230731. doi: 10.1016/j.cmi.2023.07.024. PubMed PMID: 37532127.
10. Goman A, Ize B, Jeannot K, Pin C, Payros D, Goursat C, et al. Uncovering a new family of conserved virulence factors that promote the production of host-damaging outer membrane vesicles in gram-negative bacteria. J Extracell Vesicles. 2025;14(1):e270032. doi: 10.1002/jev2.70032. PubMed PMID: 39840902.
11. David L, Taieb F, Penary M, Bordignon PJ, Planes R, Bagayoko S, et al. Outer membrane vesicles produced by pathogenic strains of Escherichia coli block autophagic flux and exacerbate inflammasome activation. Autophagy. 2022;18(12):2913-25. Epub 20220407. doi: 10.1080/15548627.2022.2054040. PubMed PMID: 35311462; PubMed Central PMCID: PMCPMC9673956.
12. Pin C, David L, Oswald E. Modulation of Autophagy and Cell Death by Bacterial Outer-Membrane Vesicles. Toxins. 2023;15(8). Epub 20230814. doi: 10.3390/toxins15080502. PubMed PMID: 37624259; PubMed Central PMCID: PMCPMC10467092.

13. Kaderabkova N, Bharathwaj M, Furniss RCD, Gonzalez D, Palmer T, Mavridou DAI. The biogenesis of beta-lactamase enzymes. Microbiology (Reading). 2022;168(8). doi: 10.1099/mic.0.001217. PubMed PMID: 35943884; PubMed Central PMCID: PMCPMC10235803.
14. Arab T, Mallick ER, Huang Y, Dong L, Liao Z, Zhao Z, et al. Characterization of extracellular vesicles and synthetic nanoparticles with four orthogonal single-particle analysis platforms. J Extracell Vesicles. 2021;10(6):e12079. Epub 20210406. doi: 10.1002/jev2.12079. PubMed PMID: 33850608; PubMed Central PMCID: PMCPMC8023330.
15. Bachurski D, Schuldner M, Nguyen PH, Malz A, Reiners KS, Grenzi PC, et al. Extracellular vesicle measurements with nanoparticle tracking analysis - An accuracy and repeatability comparison between NanoSight NS300 and ZetaView. J Extracell Vesicles. 2019;8(1):1596016. Epub 20190401. doi: 10.1080/20013078.2019.1596016. PubMed PMID: 30988894; PubMed Central PMCID: PMCPMC6450530.
16. Johnson JR, Oswald E, O'Bryan TT, Kuskowski MA, Spanjaard L. Phylogenetic distribution of virulence-associated genes among Escherichia coli isolates associated with neonatal bacterial meningitis in the Netherlands. The Journal of infectious diseases. 2002;185(6):774-84. Epub 20020214. doi: 10.1086/339343. PubMed PMID: 11920295.
17. Kunsmann L, Ruter C, Bauwens A, Greune L, Gluder M, Kemper B, et al. Virulence from vesicles: Novel mechanisms of host cell injury by Escherichia coli O104:H4 outbreak strain. Scientific reports. 2015;5:13252. doi: 10.1038/srep13252. PubMed PMID: 26283502; PubMed Central PMCID: PMC4539607.
18. Santos JC, Dick MS, Lagrange B, Degrandi D, Pfeffer K, Yamamoto M, et al. LPS targets host guanylate-binding proteins to the bacterial outer membrane for non-canonical inflammasome activation. EMBO J. 2018;37(6). Epub 20180219. doi: 10.15252/embj.201798089. PubMed PMID: 29459437; PubMed Central PMCID: PMCPMC5852652.
19. Stamenkovic M, Janjetovic K, Paunovic V, Ciric D, Kravic-Stevovic T, Trajkovic V. Comparative analysis of cell death mechanisms induced by lysosomal autophagy inhibitors. Eur J Pharmacol. 2019;859:172540. Epub 20190713. doi: 10.1016/j.ejphar.2019.172540. PubMed PMID: 31310755.
20. Bielaszewska M, Ruter C, Kunsmann L, Greune L, Bauwens A, Zhang W, et al. Enterohemorrhagic Escherichia coli hemolysin employs outer membrane vesicles to target mitochondria and cause endothelial and epithelial apoptosis. PLoS Pathog. 2013;9(12):e1003797. Epub 20131212. doi: 10.1371/journal.ppat.1003797. PubMed PMID: 24348251; PubMed Central PMCID: PMCPMC3861543.
21. Canas MA, Gimenez R, Fabrega MJ, Toloza L, Baldoma L, Badia J. Outer Membrane Vesicles from the Probiotic Escherichia coli Nissle 1917 and the Commensal ECOR12 Enter Intestinal Epithelial Cells via Clathrin-Dependent Endocytosis and Elicit Differential Effects on DNA Damage. PloS one. 2016;11(8):e0160374. Epub 20160803. doi: 10.1371/journal.pone.0160374. PubMed PMID: 27487076; PubMed Central PMCID: PMCPMC4972321.
22. Krsek D, Yara DA, Hrbackova H, Daniel O, Mancikova A, Schuller S, et al. Translocation of outer membrane vesicles from enterohemorrhagic Escherichia coli O157 across the intestinal epithelial barrier. Frontiers in microbiology. 2023;14:1198945. Epub 20230525. doi: 10.3389/fmicb.2023.1198945. PubMed PMID: 37303786; PubMed Central PMCID: PMCPMC10248468.

23. Thapa HB, Kohl P, Zingl FG, Fleischhacker D, Wolinski H, Kufer TA, et al. Characterization of the Inflammatory Response Evoked by Bacterial Membrane Vesicles in Intestinal Cells Reveals an RIPK2-Dependent Activation by Enterotoxigenic Escherichia coli Vesicles. Microbiology spectrum. 2023;11(4):e0111523. Epub 20230612. doi: 10.1128/spectrum.01115-23. PubMed PMID: 37306596; PubMed Central PMCID: PMCPMC10433812.
24. Kesty NC, Mason KM, Reedy M, Miller SE, Kuehn MJ. Enterotoxigenic Escherichia coli vesicles target toxin delivery into mammalian cells. EMBO J. 2004;23(23):4538-49. Epub 20041118. doi: 10.1038/sj.emboj.7600471. PubMed PMID: 15549136; PubMed Central PMCID: PMCPMC533055.
25. Doherty GJ, McMahon HT. Mechanisms of endocytosis. Annu Rev Biochem. 2009;78:857-902. doi: 10.1146/annurev.biochem.78.081307.110540. PubMed PMID: 19317650.
26. Kumari S, Mg S, Mayor S. Endocytosis unplugged: multiple ways to enter the cell. Cell Res. 2010;20(3):256-75. Epub 20100202. doi: 10.1038/cr.2010.19. PubMed PMID: 20125123; PubMed Central PMCID: PMCPMC7091825.
27. Macia E, Ehrlich M, Massol R, Boucrot E, Brunner C, Kirchhausen T. Dynasore, a cell-permeable inhibitor of dynamin. Dev Cell. 2006;10(6):839-50. doi: 10.1016/j.devcel.2006.04.002. PubMed PMID: 16740485.
28. Marks B, Stowell MH, Vallis Y, Mills IG, Gibson A, Hopkins CR, et al. GTPase activity of dynamin and resulting conformation change are essential for endocytosis. Nature. 2001;410(6825):231-5. doi: 10.1038/35065645. PubMed PMID: 11242086.
29. Kim OY, Hong BS, Park KS, Yoon YJ, Choi SJ, Lee WH, et al. Immunization with Escherichia coli outer membrane vesicles protects bacteria-induced lethality via Th1 and Th17 cell responses. Journal of immunology. 2013;190(8):4092-102. doi: 10.4049/jimmunol.1200742. PubMed PMID: 23514742.
30. Bomberger JM, Maceachran DP, Coutermarsh BA, Ye S, O'Toole GA, Stanton BA. Long-distance delivery of bacterial virulence factors by Pseudomonas aeruginosa outer membrane vesicles. PLoS Pathog. 2009;5(4):e1000382. Epub 20090410. doi: 10.1371/journal.ppat.1000382. PubMed PMID: 19360133; PubMed Central PMCID: PMCPMC2661024.
31. Harder T, Scheiffele P, Verkade P, Simons K. Lipid domain structure of the plasma membrane revealed by patching of membrane components. J Cell Biol. 1998;141(4):929-42. doi: 10.1083/jcb.141.4.929. PubMed PMID: 9585412; PubMed Central PMCID: PMCPMC2132776.
32. O'Donoghue EJ, Krachler AM. Mechanisms of outer membrane vesicle entry into host cells. Cellular microbiology. 2016. doi: 10.1111/cmi.12655. PubMed PMID: 27529760.
33. Kesty NC, Kuehn MJ. Incorporation of heterologous outer membrane and periplasmic proteins into Escherichia coli outer membrane vesicles. J Biol Chem. 2004;279(3):2069-76. Epub 20031024. doi: 10.1074/jbc.M307628200. PubMed PMID: 14578354; PubMed Central PMCID: PMCPMC3525464.
34. Soysal N, Mariani-Kurkdjian P, Smail Y, Liguori S, Gouali M, Loukiadis E, et al. Enterohemorrhagic Escherichia coli Hybrid Pathotype O80:H2 as a New Therapeutic Challenge. Emerging infectious diseases. 2016;22(9):1604-12. doi: 10.3201/eid2209.160304. PubMed PMID: 27533474; PubMed Central PMCID: PMC4994344.
35. Mariani-Kurkdjian P, Lemaitre C, Bidet P, Perez D, Boggini L, Kwon T, et al. Haemolytic-uraemic syndrome with bacteraemia caused by a new hybrid Escherichia coli pathotype. New

microbes and new infections. 2014;2(4):127-31. doi: 10.1002/nmi2.49. PubMed PMID: 25356358; PubMed Central PMCID: PMC4184582.

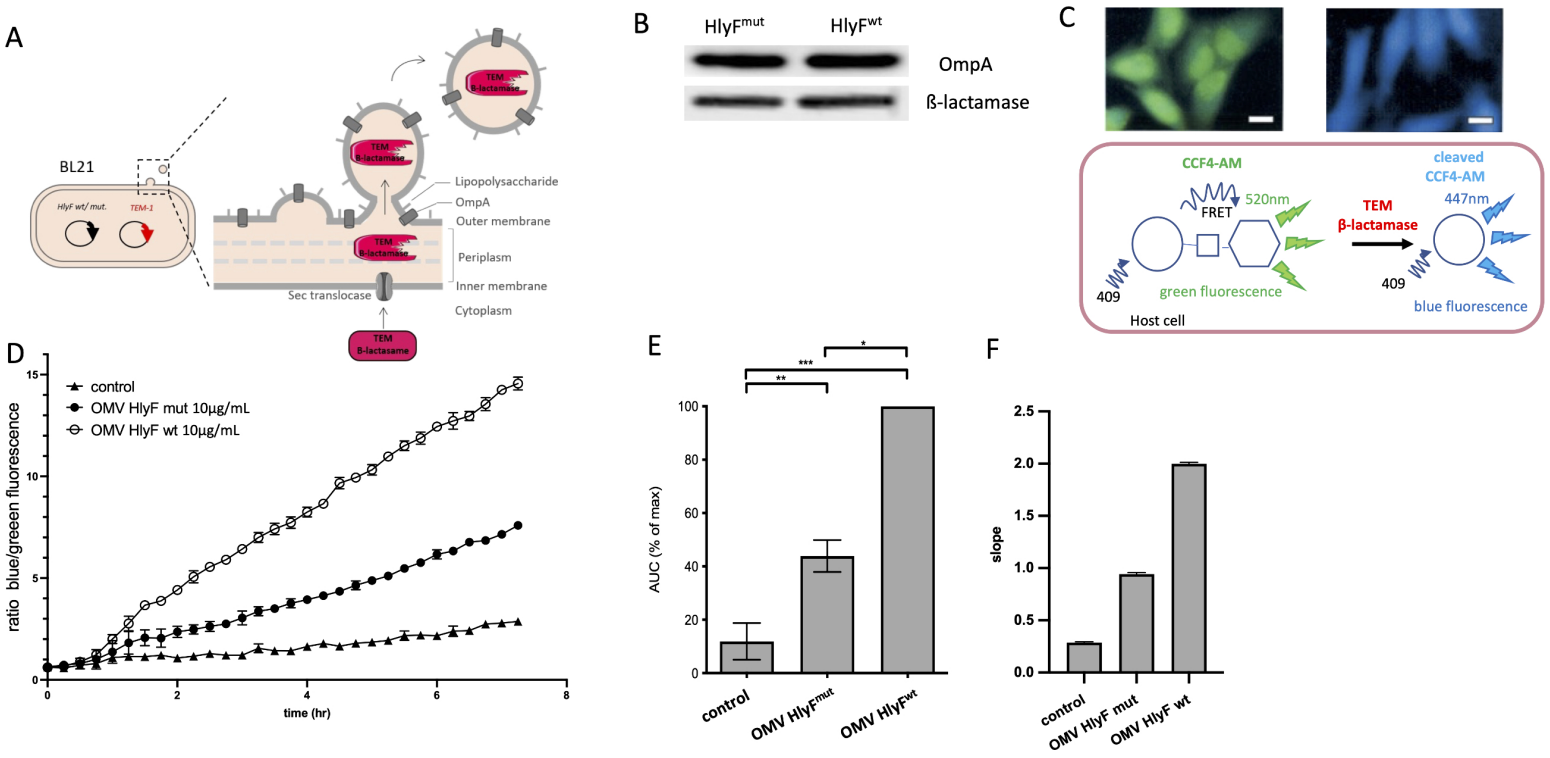
A
BL21
HlyF wt/ mut.
TEM-1
TEM
B-lactamase
Lipopolysaccharide
OmpA
Outer membrane
Periplasm
Inner membrane
Sec translocase
Cytoplasm
B
HlyF^mut
HlyF^wt
OmpA
ß-lactamase
C
CCF4-AM
520nm
FRET
green fluorescence
409
Host cell
TEM
β-lactamase
cleaved
CCF4-AM
447nm
blue fluorescence
D
control
OMV HlyF mut 10µg/mL
OMV HlyF wt 10µg/mL
ratio blue/greeen fluorescence
time (hr)
E
AUC (% of max)
control
OMV HlyF^mut
OMV HlyF^wt
F
slope
control
OMV HlyF mut
OMV HlyF wt

Figure 1

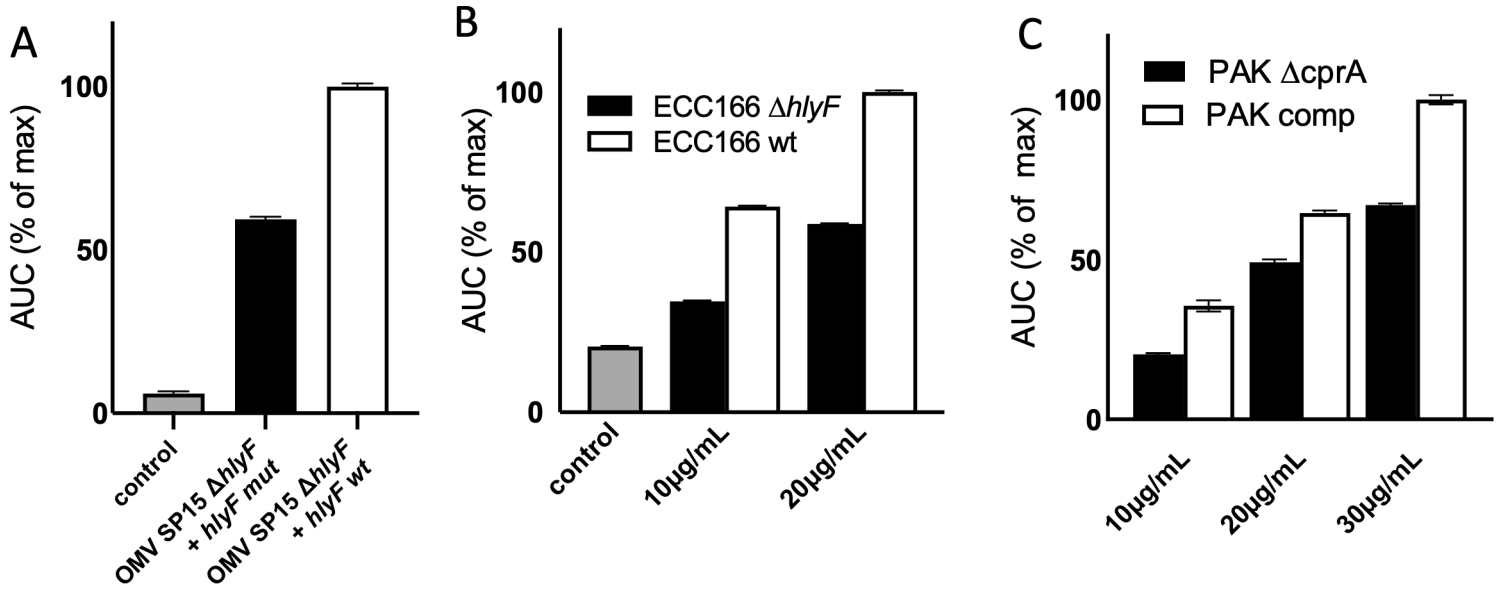
A
AUC (% of max)
100
50
0
control
OMV SP15 ΔhlyF + hlyF mut
OMV SP15 ΔhlyF + hlyF wt
B
AUC (% of max)
100
50
0
ECC166 ΔhlyF
ECC166 wt
control
10µg/mL
20µg/mL
C
AUC (% of max)
100
50
0
PAK ΔcprA
PAK comp
10µg/mL
20µg/mL
30µg/mL

Figure 2

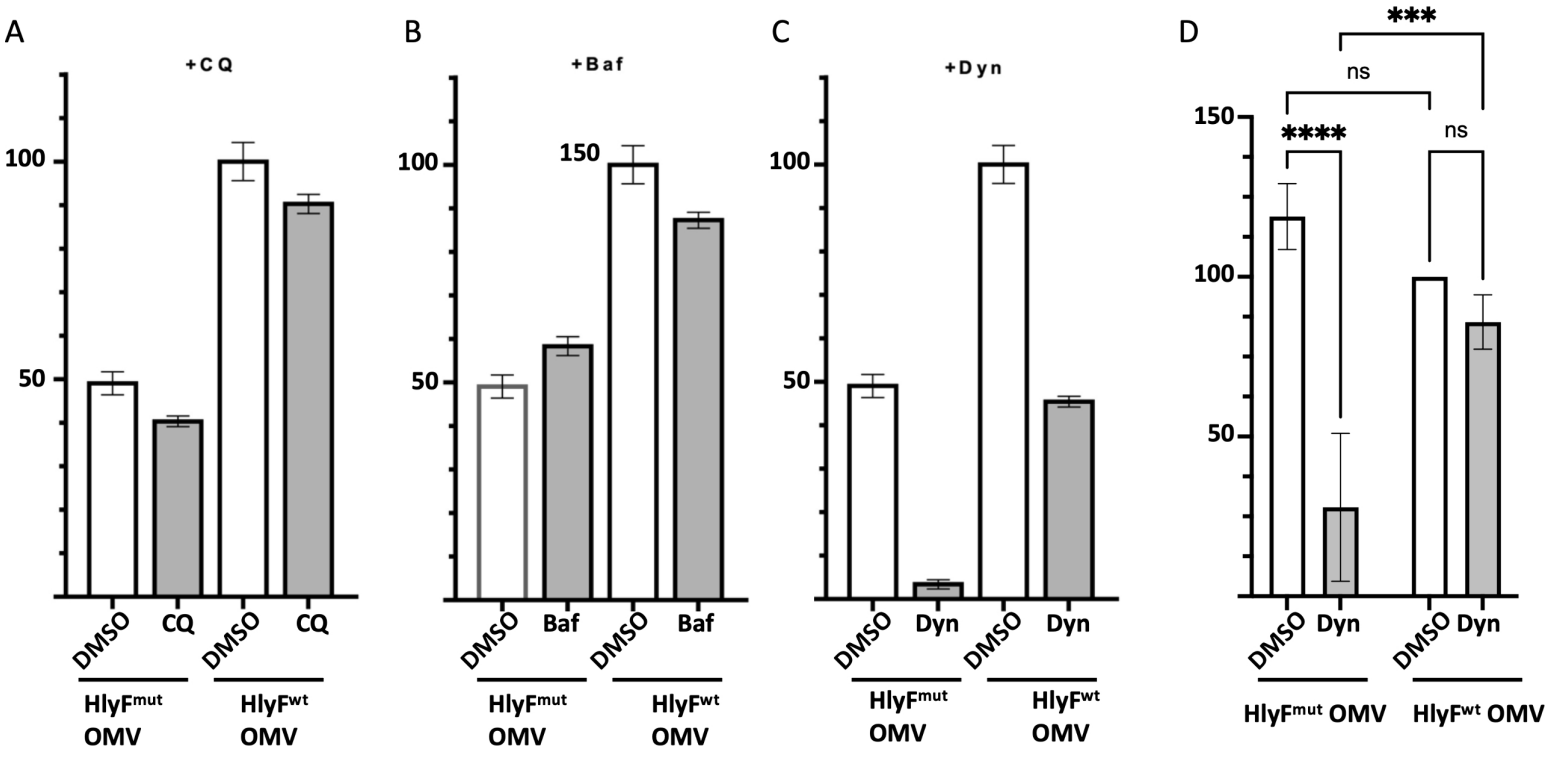
A
+CQ
100
50
DMSO
CQ
DMSO
CQ
HlyFmut OMV
HlyFwt OMV
B
+Baf
100
150
50
DMSO
Baf
DMSO
Baf
HlyFmut OMV
HlyFwt OMV
C
+Dyn
100
50
DMSO
Dyn
DMSO
Dyn
HlyFmut OMV
HlyFwt OMV
D
***
ns
****
ns
150
100
50
DMSO
Dyn
DMSO
Dyn
HlyFmut OMV
HlyFwt OMV

Figure 3

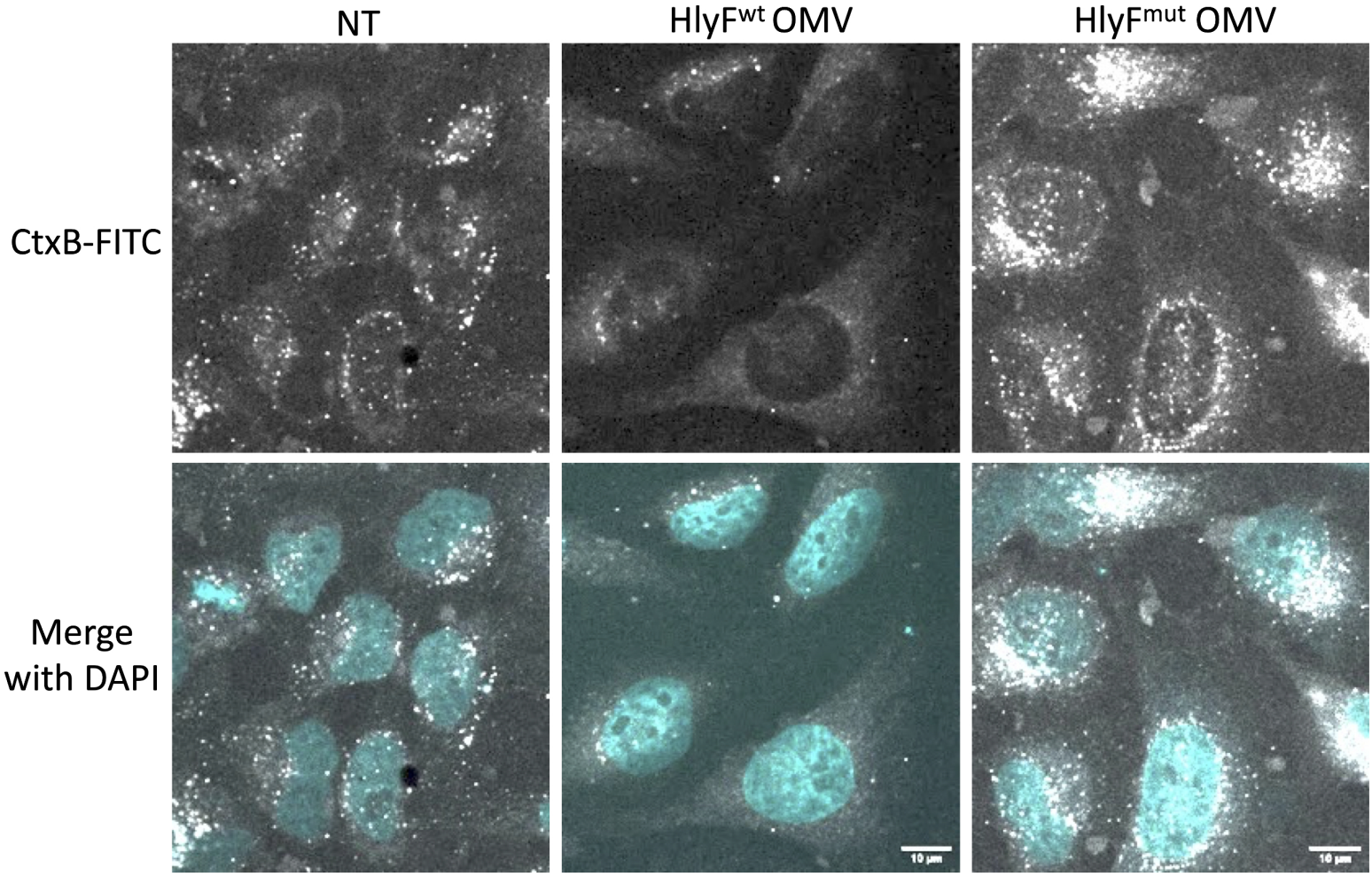
NT
HlyF^{wt} OMV
HlyF^{mut} OMV
CtxB-FITC
Merge
with DAPI
10 µm
10 µm

Figure 4

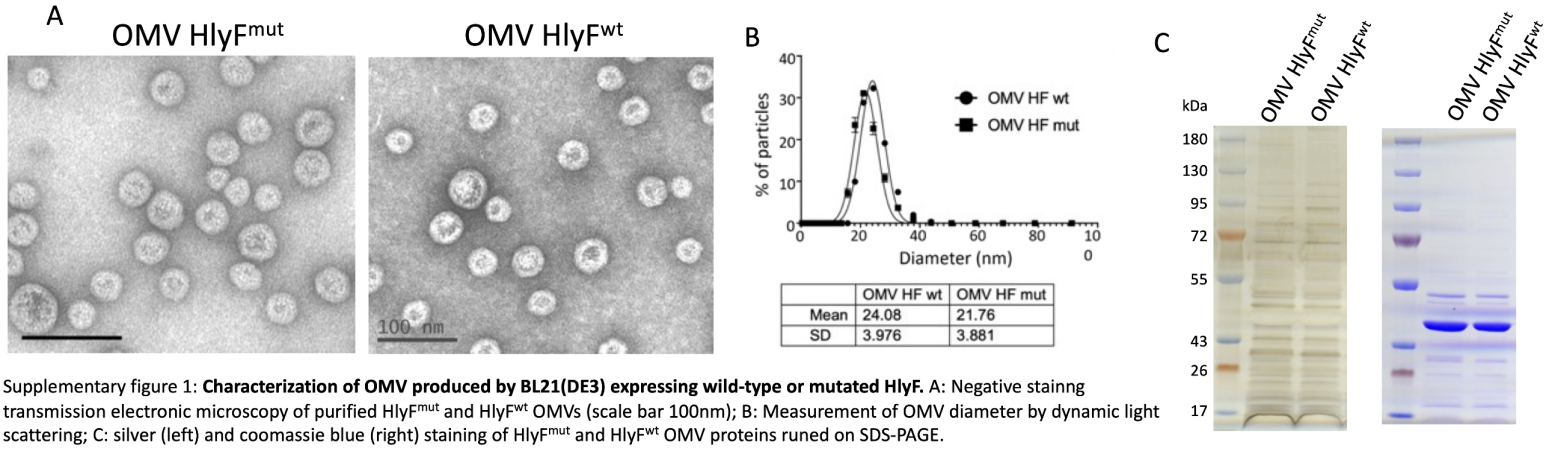

	OMV HF wt	OMV HF mut
Mean	24.08	21.76
SD	3.976	3.881

Supplementary figure 1: **Characterization of OMV produced by BL21(DE3) expressing wild-type or mutated HlyF.** A: Negative stainng transmission electronic microscopy of purified HlyF^{mut} and HlyF^{wt} OMVs (scale bar 100nm); B: Measurement of OMV diameter by dynamic light scattering; C: silver (left) and coomassie blue (right) staining of HlyF^{mut} and HlyF^{wt} OMV proteins runed on SDS-PAGE.

Supplementary file